Received: 7 May 2020 | Revised: 29 October 2020 | Accepted: 15 January 2021

DOI: 10.1002/oca.2710

RESEARCH ARTICLE

WILEY

A robust model predictive control framework for the regulation of anesthesia process with Propofol

Sotiris Ntouskas | **Haralambos Sarimveis**

School of Chemical Engineering, National Technical University of Athens (NTUA), Athens, Greece

Correspondence
Haralambos Sarimveis, School of Chemical Engineering, National Technical University of Athens (NTUA), 9 Heroon Polytechneiou Street, 15780 Zografou Campus, Athens, Greece.
Email: hsarimv@central.ntua.gr

Abstract

In this work, we present a robust Model Predictive Control (MPC) strategy based on linear matrix inequalities (LMIs) for the intravenous administration of Propofol, a drug which is used for anesthesia during surgeries. The controller is designed for a population of patients and takes into account constraints on the amount of administered drug and on the drug concentration profile. A detailed compartmental mathematical model available in the literature is adjusted to the available data and provides the future predictions of the process. In the context of the application, only the depth of anesthesia (BIS index) is assumed to be measured—as it is common in practice. The state of the system (drug amount in organs) is estimated in real-time by incorporating a state observer. The derived control scheme, along with the designed state observer are able to deal with major challenges in controlling the depth of anesthesia which are inter- and intra-patient variability, model nonlinearity, and model uncertainty. The controller is able to satisfy the divergent characteristics of the patients of the dataset, while satisfying in parallel all the imposed constraints. Moreover, we show that by considering smaller groups of patients with similar characteristics the corresponding responses are significantly improved.

KEYWORDS

compartmental/PBPK modeling, intravenous anesthesia, robust model predictive control

1 | INTRODUCTION

1.1 | Background

Anesthesia is a typical process during a surgery and/or in intensive care units. The purpose of regulation of anesthesia is to guarantee hypnosis, analgesia, and muscle relaxation. The process of anesthesia captured the attention of control engineers due to challenging issues that arise such as: inter- and intra-patient variability, multivariable characteristics, variable time delays, dynamics dependent on the hypnotic agent, model analysis variability, agent, and stability issues.[1-5]

There is no golden rule for achieving and maintaining unconsciousness and usually, anesthesiologists monitor hemodynamic signals and manually control the administration of the anesthetic agent in an open-loop fashion. Administered doses are determined based on an empirical estimation of the response of the patient over a future time horizon. Manual control may cause over-dose or under-dose of the anesthetic agent which are both undesired and unsafe for the patient.[6]

Automation and optimization of the delivery of anaesthetic drugs would pave the way toward safe healthcare, less prone to excessive over-dosages and under-dosages often resulting in side effects and risk of awareness. For the purpose

of automating the process of anesthesia, numerous control schemes have been proposed over the last years.[7-9] Many automated drug delivery methodologies use the proportional-integral-derivative (PID) architecture.[3,10-15] The main drawback of these controllers is that they cannot anticipate the response of the patient. Moreover they do not have any prior knowledge of the drug metabolism, so the performances are sub-optimal.

Model-based control (MBC) schemes can overcome this limitation, by including dynamic mathematical models that describe the underlying processes within the human body. Various MBC approaches have been proposed, using fuzzy control[16] adaptive control,[17-19] model based PID controllers[20] and model predictive control (MPC).[4,21-23] More recently, an extension[24] on the usual MPC studies on anesthesia, considers simultaneous administration of Propofol and remifentanil in order to gain control on the analgesic-hypnotic balance. MPC algorithms have the important advantage that can explicitly take into account constraints on the manipulated and on the controlled variables in the formulation of the optimisation problem that is solved at each discrete time instance. Multiparametric MPC solves offline the optimisation problem using multiparametric programming and derives the control inputs as a set of explicit functions of the system states.[4]

Most MBC methodologies aim to design controllers by assuming a nominal linear time-invariant (LTI) model to predict the future behavior of the system. The challenge of taking into account inter-patient variability has been emphasized in the scientific literature.[25] Robustness on inter and intra-patient variability has been studied by applying the same controller to patients with different characteristics from the nominal patient or by using robustness tests after the controller has been designed.[21] In Reference 22, an individualised physiologically-based pharmacokinetic (PBPK) modeling approach is proposed. The PBPK model is adapted to the individual physiological characteristics, and practically a different controller is designed for each patient. These references in literature reveal the need of an administration strategy, robust enough to deal with inter- and intra- patient variability, and the individualized characteristics of each patient.

1.2 | Contributions

In this article, we are studying the problem of robust MPC control of anesthesia, by considering the patient variability explicitly in the design phase. The problem has been addressed in Reference 26 where a mixed H_2/H_∞ controller is proposed to robustly control a population of patients. But in this methodology, no input or output constraints are incorporated.

In this work, we are applying the robust MPC strategy using linear matrix inequalities (LMIs) described in details in Reference 27. Mathematical models of a group of virtually generated realistic patients represent the model uncertainty during the anesthesia process. These models are based on a statistical analysis on inter-patient variability[28] as described in References 6 and 29. Moreover, it is assumed that only the output of the system is measured, that is, the quantified expression of the depth of anesthesia. In order to get an accurate estimation of the state vector of the system, namely the amount of the drug over the various compartments, a state observer is incorporated.

The main outcome of this article is the derivation of a robust control law that can be applied for the derivation of the administered dose over the entire population or subpopulations, while satisfying drug administration and drug concentration constraints. This way we derive generic control laws—optimal over populations of patients—to achieve the desired depth on anesthesia, while in parallel, the imposed constraints are satisfied. Moreover a Kalman filter is incorporated to get accurate knowledge of the unmeasured state vector of the system, at each instant of the simulation.

As mentioned in the previous subsection, a number of MPC based approaches have addressed the problem of regulating the depth of anesthesia (DOA). Many of them, consider the problem from a multi-parametric point of view.[4,30-32] There are also relative papers where state estimation is incorporated.[33,34]

The advantage of the proposed methodology is robustness to model uncertainty and noise. Namely, instead of knowing the exact model of a patient, it suffices that the characteristics of the patient lie in the convex hull of a group of known patients, for which the control law has been designed. By considering smaller groups of similar patients, the controller achieves rapidly the desired depth of anesthesia. The incorporation of a state observer completes a realistic setup for usage during a typical surgery.

The article is structured as follows: In Section 2, the mathematical model used to describe the process of anesthesia is presented. In Section 3, we describe the methodology of robust infinite-horizon MPC based on LMIs for systems with polytopic uncertainty. Moreover a short description of state estimation is presented with special focus on *Kalman filter*. Finally, in Section 4, the robust infinite-horizon MPC for the control of anesthesia is applied to a dataset of patients using Propofol, as the anesthetic agent. It is illustrated that the MPC control strategy achieves the desired set-points and

satisfies the imposed constraints for all patients in the dataset. It is also demonstrated that similar results are obtained after applying the same control law to additional patients, with the only requirement that they belong to the convex hull of the original dataset. It is shown that the desired setpoints are achieved during both the induction and maintenance phases, with the ability of rejecting disturbances while maintaining the imposed constraints.

2 | MODELING OF INTRAVENOUS ANESTHESIA

The drugs used to induce anesthesia can be either gases/vapors, such as desflurane, sevoflurane, and isoflurane[7] or are injected intravenously as in case of Propofol[6] and Etomidate.[35,36] Intravenous administration is consider to induce anesthesia smoother and much faster. For the intravenous anesthesia, Propofol[6] is used as the standard agent, using electronically controlled intravenous infusion pumps. For measuring the effect of Propofol administration, various methods have been developed,[37] but the bispectral index (BIS) method is the most popular and widely used.[7] The BIS index makes use of a signal derived from the electro-encephalogram (EEG).[38] The BIS algorithm gets this signal in a complex formula as referred in Reference 39 with advanced artifact rejection techniques, and produces a dimensionless number between 0 and 100, which measures the level of consciousness during anesthesia. Range 90-100 corresponds to a fully awake patient, while ranges 60–70 and 40–60 represent light and moderate hypnotic state, respectively.

2.1 | Pharmacokinetics/pharmacodynamics model

In Figure 1, the compartmental model of the patient is presented containing the pharmacokinetic (PK) and the pharmacodynamic (PD) models, where in each compartment, the drug concentration is assumed to be uniform, as in a perfect and instantaneous mixing. The state space model is described by a system of ordinary differential equations (ODEs),[6,30] as depicted in (1):

$$\dot{x_1}(t) = -\left[k_{10} + k_{12} + k_{13}\right] \cdot x_1(t) + k_{21} \cdot x_2(t) + k_{31} \cdot x_3(t) + u(t) \tag{1a}$$

$$\dot{x_2}(t) = k_{12} \cdot x_1(t) - k_{21} \cdot x_2(t) \tag{1b}$$

$$\dot{x_3}(t) = k_{13} \cdot x_1(t) - k_{31} \cdot x_3(t) \tag{1c}$$

$$\dot{x_e}(t) = k_{1e} \cdot x_1(t) - k_{e0} \cdot x_e(t) \tag{1d}$$

where x_1 (mg) denotes the amount of drug in the central compartment namely the intravascular blood. The corresponding blood concentration is denoted as C_1 and is equal to x_1/V_1, where V_1 is the volume of the compartment 1 namely the blood. The Compartments 2 (muscle) and 3 (fat) model the drug exchange of the blood with well and poorly diffused body tissues. The masses of drug in these peripheral compartments are denoted by x_2 and x_3, respectively. The coefficients k_{ij} for $i \neq j$ denote the drug transfer frequency from the i^{th} to the j^{th} compartment and $u(t)$ is the infusion rate of the anaesthetic drug into the central compartment. In general, the parameters of k_{ij} depend on age, weight, height, and gender.[30,40]

In order to simulate the lag between drug concentration and the drug response, a hypothetical effect compartment is added at the compartmental representation of the system. Its corresponding drug concentration is denoted by C_e and

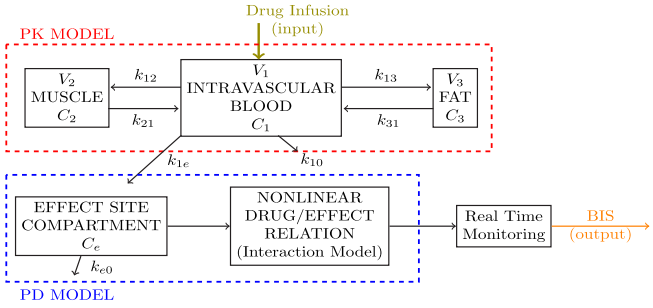

FIGURE 1 Compartmental model presenting the pharmacokinetic (PK) and the pharmacodynamic (PD) models of the patient[6] [Colour figure can be viewed at wileyonlinelibrary.com]

in Reference 30 and in Reference 6 is referred as the *effect-site compartment*. The mass of the drug at this compartment is considered to be the last element of the state vector denoted by x_e. This theoretical effect compartment receives drug from the central compartment by a first-order process and in clinical practice it is considered that the transfer frequency for Propofol from the central compartment to the effect compartment is equal to the removal frequency from the effect compartment. Thus, in Equation (1), it is considered that $k_{e0} = k_{1e}\ (\text{min}^{-1})$.[41-43]

The pharmacodynamic model relates the BIS index to the concentration of the anaesthetic agent C_e by the empirical static but time varying nonlinear Equation (2), which is also known as the Hill curve:[29,44]

$$BIS(t) = E_0 - E_{max} \cdot \frac{C_e^{\gamma_1}(t)}{C_e^{\gamma_1}(t) + EC_{50}^{\gamma_1}}. \tag{2}$$

In Equation (2), E_0 denotes the BIS value in a fully awake state, which by convention is equal to 100. E_{max} represents the maximum effect achieved by the drug infusion, EC_{50} denotes the drug concentration at the 50% of the maximal effect, which in essence is the measure of the sensitivity of the patient to the drug. Finally, the value of γ_1 determines the steepness of the Hill curve. If we solve Equation (2) for $C_e(t)$, the following nonlinerar equation is obtained:[21,41-43,45]

$$C_e(t) = EC_{50}\left(\frac{E_0 - BIS(t)}{E_{max} - E_0 + BIS(t)}\right)^{\frac{1}{\gamma_1}}. \tag{3}$$

Derivation of Equation (3) illustrates that the function defined in Equation (2) is invertible, that is, it is strictly monotonic and there is 1-1 correspondence between C_e and BIS, meaning that each C_e value is mapped to a single BIS value and vice versa. Therefore, the Hill curve function and more specifically, Equation (3) is used only to define the set-point for C_e given a desired BIS value and the linear state space model is adequate for designing the controller.

2.2 | Patients population

Equations (1) and (2) constitute a generic PK-PD model for the administration of Propofol to patients, but the specific parameter values in these models differ among patients, due to different sensitivities to Propofol. Sensitive patients are modeled by lower drug transfer coefficients from intravascular blood to muscle, fat and the effect site compartments, k_{10}, k_{12}, k_{13}, and by higher k_{21} and k_{k31} values. As far as PD parameters are concerned, sensitive patients are modeled by lower EC_{50} indicating the need for smaller drug doses to achieve the desired hypnotic results and by lower γ_1 values. Therefore, a different continuous state-space model of the form of Equation (1) is used to describe each patient, which can be converted to the discrete-time counterpart assuming *zero-order hold*:[46]

$$x(k+1) = A_j x(k) + B_j u(k) \tag{4a}$$

$$y(k) = Cx(k) \tag{4b}$$

where $j \in 1, 2, \ldots, L$, L is the number of patients, $u(k)$ is the infusion rate of Propofol, $x(k) = [x_1(k), x_2(k), x_3(k), x_e(k)]^T$ is the state vector, and $y(k) = x_e(k)$ is the output of the system at the discrete time instant k.

3 | ROBUST INFINITE HORIZON MPC WITH POLYTOPIC UNCERTAINTY

3.1 | Polytopic uncertainty or multimodel systems

The uncertainty of the system of patients which is due to different state-space models of the form of Equation (4) can be described by considering the following discrete-time linear time invariant (LTI) system:

$$x(k+1) = Ax(k) + Bu(k) \tag{5a}$$

$$y(k) = Cx(k) \tag{5b}$$

$$\begin{bmatrix} A & B \end{bmatrix} \in \Omega \tag{5c}$$

where $u(k) \in \mathbb{R}^{n_u}$ is the control input, $x(k) \in \mathbb{R}^{n_x}$ is the state vector, $y(k) \in \mathbb{R}^{n_y}$ is the output of the system, and Ω is a polytope defined by the convex hull of the matrices $A_j, B_j, j \in 1, 2, \ldots, L$:

$$\Omega = Co\left\{ \begin{bmatrix} A_1 & B_1 \end{bmatrix}, \quad \begin{bmatrix} A_2 & B_2 \end{bmatrix}, \quad \ldots, \quad \begin{bmatrix} A_L & B_L \end{bmatrix} \right\}. \tag{6}$$

According to Equation (6) when model uncertainty is present, the exact model $\begin{bmatrix} A & B \end{bmatrix}$ is unknown. Instead it is sufficient to know that the model belongs to the convex hull described by Equation (6) or alternatively it should hold that $\begin{bmatrix} A & B \end{bmatrix} = \sum_{j=1}^{L} \lambda_j \begin{bmatrix} A_j & B_j \end{bmatrix}, \sum_{j=1}^{L} \lambda_j = 1, \lambda_j \geq 0, \forall j$.

3.2 | Robust model predictive control using linear matrix inequalities

3.2.1 | Unconstrained problem

In this section, we present the problem formulation for the unconstrained problem of the robust MPC using LMIs as it is presented in Reference 27. Extensive references for the use of LMIs in formulation of robust MPC can be found in References 47-51. In this approach, instead of minimizing a nominal objective function, we consider one objective function for each patient and then minimize the *worst-case* objective function for the case of *infinite-horizon MPC* problem. At first the unconstrained problem is described and next input and output constraints are incorporated. Given the state-space model described by Equations (5) and (6), the problem of minimizing the worst-case objective function is formulated next:

$$\min_{u(k+i|k), i=0,1,\ldots,m} \max_{[A\ B]\in\Omega} J_\infty(k) \tag{7}$$

where

$$J_\infty(k) = \sum_{i=0}^{\infty} \left[x(k+i|k)^T Q_1 x(k+i|k) + u(k+i|k)^T R u(k+i|k) \right] \tag{8}$$

and $Q_1 > 0, R > 0$ are the weighting matrices. The notation $x(k+i|k)$ corresponds to the state vector at time $k+i$, predicted based on measurements at k, for $i = 0, 1, 2, \ldots$; $u(k+i|k)$ is the control move at time $k+i$, computed by the optimization problem based on measurements at k, for $i = 0, 1, 2, \ldots m$; and m is the control horizon. It is assumed that there is no control action after time instant $k+m$, that is, $u(k+i|k) = 0, i > m$.

This *min-max* problem over the set Ω ensures that the reference model used for predictions is the one that leads to the largest or worst-case value of J_∞ among all systems $\in \Omega$. This problem is not computationally tractable especially as the number of LTI systems increases. Instead the problem of formulating Equation (8) is addressed in Reference 27 by deriving an upper bound on the robust performance objective. Then this upper bound is minimized resulting in a control law with constant state feedback gain of the form:

$$u(k+i|k) = F \cdot x(k+i|k), \quad i \geq 0. \tag{9}$$

For the calculation of the upper bound a quadratic function of the form $V(x) = x^T P x$ of the state is used[27] with $P > 0$ and $V(0) = 0$. At each sampling time k, suppose V for any system contained in Ω satisfies:

$$V(x(k+i+1|k)) - V(x(k+i|k)) \leq -\left[x(k+i|k)^T Q_1 x(k+i|k) + u(k+i|k)^T R u(k+i|k) \right]. \tag{10}$$

The sum of terms of Equation (10) from $i = 0$ to ∞ is equal to:

$$-V(x(k|k)) \leq -J_\infty(k). \tag{11}$$

So function $V(x) = x^T P x$ could be considered as an upper bound of the cost function of the systems contained in Ω, that is,

$$\max_{[A\ B]\in\Omega} J_\infty(k) \leq V(x(k|k)). \tag{12}$$

Consequently, for the purposes of robust MPC, it is sufficient to minimize the upper bound of the objective functions.[27] The outcome of this minimization problem at each time step k is a constant state-feedback control law $u(k+i|k) = F \cdot x(k+i|k)$. As it is common practice in MPC theory, only the first computed input $u(k|k) = F \cdot x(k|k)$ is implemented. At the next time instant, the state vector $x(k+1)$ is computed again and is used as input to formulate again the optimization problem, and the procedure is repeated. The following theorem gives the conditions for the existence of the appropriate $P > 0$ and the corresponding state feedback matrix F as it is given in Reference 27:

Theorem 1. *Let $x(k) = x(k|k)$ be the state of an uncertain system described in Equation (1), measured at sampling time k. Assume that there are no constraints on the control input and system's output. Moreover suppose that the uncertainty lies in a polytopic set Ω as in Equation (6). Then the state feedback matrix F in the control law $u(k+i|k) = F \cdot x(k+i|k), i \geq 0$ that minimizes the upper bound $V(x(k|k))$ on the robust performance objective function at sampling time k is given by:*

$$F = Y \cdot Q^{-1} \tag{13}$$

where $Q > 0$ and Y are obtained from the solution (if it exists) of the following linear objective minimization problem:

$$\min_{\gamma,Q,Y} \gamma \tag{14}$$

subject to:

$$\begin{bmatrix} 1 & x(k|k)^T \\ x(k|k) & Q \end{bmatrix} \geq 0 \tag{15}$$

and

$$\begin{bmatrix} Q & QA_j^T + Y^T B_j^T & QQ_1^{1/2} & Y^T R^{1/2} \\ A_j Q + B_j Y & Q & 0 & 0 \\ Q_1^{1/2} & 0 & \gamma I & 0 \\ R^{1/2} T & 0 & 0 & \gamma I \end{bmatrix} \geq 0, \quad j = 1, 2, \ldots, L. \tag{16}$$

The proof of theorem above is given in Reference 27. According to this theorem, the solution of the robust MPC problem, that is, the minimization of the upper bound of the objective functions, is redefined in solving a simple minimization problem based on a system of two LMIs. LMI problems can be solved in polynomial time, which means that they have low computational complexity. Nowadays, there are effective and powerful algorithms that they can compute the global optimum very fast, with non-heuristic stopping criteria. This is the reason why transformation of optimal control problems to LMI formulations is an attractive approach.[52] Problems of LMIs are usually cast as *Semidefinite Program* (SDP) problems, which in turn are transformed to cone programs with no second-order cone constraints. Solution of this type of problems leads to the solution of a pair of primal and dual cone programs. For an in-depth review in LMI-based optimization theory and applications, reader is referred to Reference 53. In Reference 27 it has been proved that the feasible receding horizon state feedback control law defined by Equations (13)–(16) (Theorem 1) robustly asymptotically stabilizes the closed-loop system.

3.2.2 | Constrained problem

In many practical applications, input and output constraints are imposed. This also holds for the anesthesia process. An upper bound is imposed on the infusion rate of the intravenous infusion pump due to physical limitation of the process equipment. A lower bound is imposed on the BIS index because an excessive degree of anesthesia (as a result of very low value of BIS index) causes severe side effects and longer recovery times. This constraint is translated to an upper bound on the actual output $x_e(k)$ of the state space system (4), using Equation (3).

According to Reference 27, the input constraint for a single input variable at each sampling time k, can be described by the following equation:

$$|u(k+i|k)| \leq u_{max}, \quad i \geq 0. \tag{17}$$

It should be noted here that input constraints are imposed over the entire future horizon input sequence, although only the first control input $u(k|k) = u(k)$ is implemented. By referring to Reference 53, constraint (17) could be transformed to:

$$\begin{bmatrix} u_{max}^2 & Y \\ Y^T & Q \end{bmatrix} \geq 0. \tag{18}$$

Similarly, for a single output variable, the output constraints can be expressed by the following inequality:

$$\max_{[A\ B]\in\Omega} |y(k+i|k)| \leq y_{max}, \quad i \geq 1. \tag{19}$$

This is a worst-case constraint over the set Ω and is imposed strictly over the future prediction horizon ($i \geq 1$). As it is shown in Reference 27 based on Reference 53, constraint (19) can be written as:

$$\begin{bmatrix} Q & (A_jQ + B_jY)^T C^T \\ C(A_jQ + B_jY) & y_{max}^2 \end{bmatrix} \geq 0, \quad j = 1, 2, \ldots, L. \tag{20}$$

Condition (20) represents a set of LMIs in Y and $Q > 0$.

3.2.3 | Constant set-point tracking

The analysis presented up to this point addresses the problem of an infinite horizon regulator with zero tracking. For the purposes of the application presented here, this is not sufficient. Instead, the system output $x_e(k)$ is required to achieve a desired steady-state r_s different from the origin, given that system matrices A and B are constant and lie in the convex hull Ω, that is, $\begin{bmatrix} A & B \end{bmatrix} \in \Omega$. The system at steady state is described by:

$$x_s = A \cdot x_s + B \cdot u_s \tag{21a}$$

$$y_s = C \cdot x_s, \tag{21b}$$

under the assumption that x_s, u_s, and y_s are feasible. The steady state vectors x_s and u_s can be calculated *off-line* by solving the linear system:

$$\begin{bmatrix} A - I & B \\ C & 0 \end{bmatrix} \cdot \begin{bmatrix} x_s \\ u_s \end{bmatrix} = \begin{bmatrix} 0 \\ r_k \end{bmatrix}. \tag{22}$$

The cost function can be written as follows:[27,54]

$$J_\infty(k) = \sum_{i=0}^{\infty} \left\{ \left[Cx(k+i|k) - Cx_s\right]^T \cdot W_1 \cdot \left[Cx(k+i|k) - Cx_s\right] + \left[u(k+i|k) - u_s\right]^T \cdot R \cdot \left[u(k+i|k) - u_s\right] \right\}$$
$$W_1 > 0, R > 0. \tag{23}$$

By defining the deviation vectors, $\tilde{x}(k) = x(k) - x_s$, $\tilde{u}(k) = u(k) - u_s$ and $\tilde{y}(k) = y(k) - y_s$, which are equal to the full vectors minus the vectors at steady state, the cost function can be written in the form of Equation (8):

$$J_\infty(k) = \sum_{i=0}^{\infty} \left\{ \left[\tilde{x}(k+i|k)\right]^T \cdot C^T W C \cdot \left[\tilde{x}(k+i|k)\right] + \left[\tilde{u}(k+i|k)\right]^T \cdot R \cdot \left[\tilde{u}(k+i|k)\right] \right\} \tag{24}$$

by considering $Q_1 = C^T WC$. The input and output constraints are modified accordingly:

$$|\tilde{u}(k+i|k)| \leq u_{max} - u_s, \quad i \geq 0 \tag{25}$$

$$\max_{[A\ B]\in\Omega} |\tilde{y}(k+i|k)| \leq y_{max} - y_s, \quad i \geq 1. \tag{26}$$

Therefore, the complete set-point tracking problem is presented in a form where we can apply Theorem 1 with the addition of LMIs (18) and (20).

3.3 | State estimation

Quite often in drug administration applications, the knowledge of the quantities of the drug over the various compartments during treatment, is completely or partially missing.[55] In order to handle the lack of such critical data, it is requisite to design a state observer.[56] A state observer is a dynamical system whose aim is to provide estimates for the (unmeasured) state vector of the patient dynamics. The information required as input to the state observer is the input applied to the system (the drug administration rate) and the corresponding output, in our case the BIS index[57] or alternatively the concentration of Propofol in the *effect-site compartment* $x_e(k)$. Requirement for the application of a state observer is the system to be *observable*, that is, the rank of the observability matrix to be equal to the number of state variables.

The type of state observer chosen for the current application is the discrete *Kalman filter*. Kalman filter optimally addresses the problem of estimating the state vector $x \in \mathbb{R}^n$ of a process governed by a linear equation of the form:

$$x(k+1) = Ax(k) + Bu(k) + w(k) \tag{27a}$$

$$y((k) = Cx(k) + v(k). \tag{27b}$$

The random variables $w(k)$ and $v(k)$ are used to model the process and measurement noise, respectively, and they are assumed to be independent on each other, white and with normal probability distributions, that is,

$$p(w) \sim \mathcal{N}(0, Q_{kalman}) \tag{27c}$$

$$p(v) \sim \mathcal{N}(0, R_{kalman}). \tag{27d}$$

A detailed description of the Kalman filter methodology is beyond the scope of this article, and the interested reader can refer to various resources on the subject, as in References 58 and 59.

In a nutshell, Kalman filter performs its estimates in a two-step process: *time update* step and *measurement update* step. During the time update step, the observer performs a-priori estimates on the system state and the error covariance matrix. Next, on the measurement update step, the observer enriches the a-priori estimations with the new measurements, to obtain improved a-posteriori estimates.

Based on the description above, the Kalman filter can be classified as a *predictor-corrector* algorithm as illustrated in Figure 2.

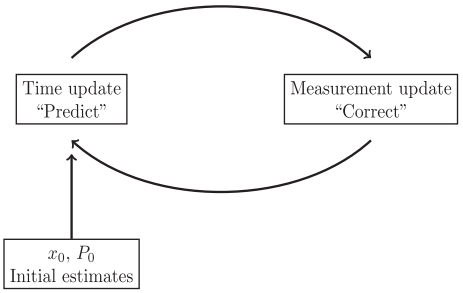

FIGURE 2 Kalman Filter iterative functionality. On time update step, filter estimates state ahead in time. Next, on measurement step, estimates are adjusted by the incoming measurements

As long as (C, A) is observable, the observer should be *asymptotically stable*, that is, for a constant input u, the observer's error defined as $\varepsilon(k) = \hat{x}(k) - x(k)$, satisfies the condition $\|\varepsilon(k)\| \to 0$ as $k \to \infty$.

4 | APPLICATION: ROBUST MPC SCHEME FOR THE CONTROL OF THE PROCESS OF ANESTHESIA

In this section, the proposed unconstrained and the constrained robust MPC methodologies are applied to the problem of controlling anesthesia in a diverse group of $L = 17$ different patients, which was originally presented in Reference 6. The patients, in broad lines, are classified in decreasing order of their BIS sensitivity to the infused amount of Propofol. So patients with lower values of ID (e.g., $ID = 1$) are considered to be more sensitive to Propofol infusion and therefore a relatively smaller amount of the drug would be sufficient to achieve the desired setpoint. On the other hand, patients with higher ID values (e.g., $ID = 17$) are considered to be insensitive in general and would require relatively larger amount of Propofol for the desired effect. Patient with number (ID) equal to 1 is considered to be the most sensitive patient, and he is used as the reference patient. The continuous state-space models described by equation 1 are converted to their discrete time counterparts (Equation 4) for all 17 patients assuming *zero-order hold*.[46] The full discrete time state-space models for all 17 patients are presented in Appendix A.

4.1 | Application of unconstrained MPC

The main objective in MPC is to drive the BIS index for all patients to the desired set-point of 50. The setup of the administration loop is as follows: At first, the state observer provides an estimate of the state vector of the system, that shall be used as input by the MPC controller. Next, according to MPC principles, the optimization problem is solved at each discrete time instant and the outcome is a sequence of optimal inputs along a future horizon. From this sequence, only the first element is applied. At the next time instant the state of the system is updated and the problem is formulated and solved all over again. The control loop is depicted in Figure 3.

The pool of the patients of the dataset is quite diverse. For this reason, the MPC should be rather conservative in its actions, in order to satisfy all the (possibly) conflicting requirements for each one of them. To this end, the matrices Q_1 and R have been selected as diagonal matrices of size 4 and 1 and their diagonal elements are equal to 10^{-4} and 10^{-1}, respectively.

Despite the fact that C_e and BIS index are correlated by the non-linear relation (2), the proposed control scheme actually considers the output of the system to be the concentration of the drug in the effect-compartment C_e instead of BIS index. This is achieved by the inverse transformation of the desired level of anesthesia in terms of BIS index into the desired level of Propofol concentration in effect compartment using Equation (3). Calibration of Kalman Filter parameters has a critical influence on its performance, especially regarding process noise covariance (Q_{Kalman}). Too small Q_{Kalman} values means that measurements are somehow untrustworthy resulting in significant lag. On the other hand, if Q_{Kalman} is too large then predictions will be closer to measurements, resulting in noisy estimations. In the presented example, it is assumed that there is quite confidence in sensors measurements, so corresponding values are $R_{Kalman} = [100]$ and Q_{Kalman} is a diagonal matrix of appropriate dimensions and diagonal elements equal to 10^4. Inequality (16) is formulated by considering all 17 patients in the dataset, that is, the discrete matrices A_j and B_j for $j = 1, \ldots, L$. The steady state vectors x_{js} and u_{js} for each patient j were calculated off-line by solving the linear system described in Equation (22).

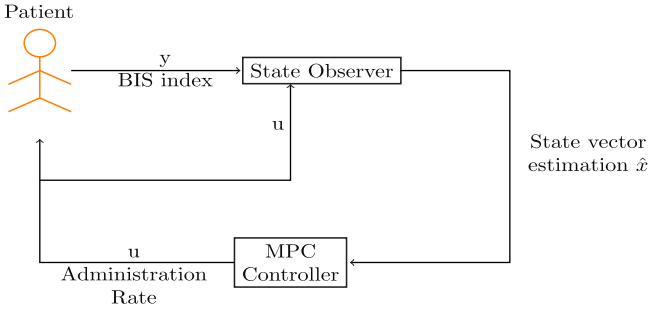

FIGURE 3 Suggested administration loop. State observer (Kalman Filter) uses current output (BIS index) and current input to estimate future state of the system on next time instant and feeds MPC. Then, the controller calculates optimal input (administration rate) to be applied to the patient and then the loop is repeated [Colour figure can be viewed at wileyonlinelibrary.com]

The time length of the simulation was set to 20 minutes, and measurements were taken every second. So at each second, the state of the system is re-evaluated, the robust MPC optimization problem is solved and the new optimal input is applied. The setpoint for the BIS index is set equal to 50. Patient No.1 is considered as the nominal patient and according to his characteristics, he is the most sensitive to Propofol among all 17 patients in the dataset,[6] that is, the patient who most likely violates the lower bound of the BIS index.

The results are shown separately for the nominal patient and then for the full set of 17 patients. Figure 4 depicts the optimal Propofol dosing trajectory for the nominal patient derived by the solution of the zero-tracking problem. All next figures referring to the input trajectory, also present solutions for the zero-tracking problems. The true dosing schemes are produced by adding the steady state input, which ranges between 8.6 and 34 mg/min for the 17 diverse patients. In Figure 5, the estimated and the actual output of the system are depicted ($\hat{C}_e$ and C_e, respectively). As it is shown in the magnified region, not highly accurate initial estimations finally converge to the actual values of the system's output. This shows that the state observer is a reliable tool for providing accurate and valid state estimations to the MPC scheme. Figure 6 presents the *BIS* index as functions of time. A red dashed line indicates the $BIS = 40$ level, which will be considered as a low bound for the Propofol administration in the constrained MPC problem that will be studied next. It is clear that this bound is violated when no constraints are assumed in the formulation of the control problem.

Figure 7 contains the BIS index responses for all 17 patients, assuming that they are administered dosages based on the optimal dosing scheme for patient No. 1. The $BIS = 40$ level and the $BIS = 50$ setpoint are shown with a red dashed line and a blue continuous line, respectively. We can notice that the responses for patients with $ID = 1, 2, 3, 4$ do violate the lower bound of BIS index. This is expected, because these patients are the most sensitive to Propofol, so the administered dose of the drug acts very drastically, resulting in low values of BIS index at the beginning of the simulation.

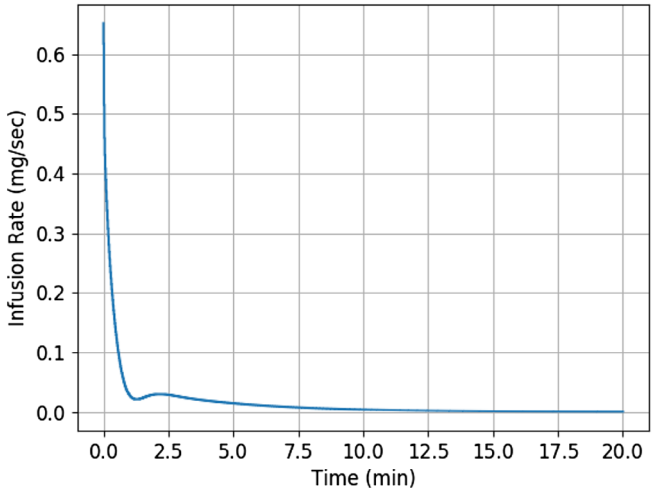

FIGURE 4 Optimal Propofol administration for the nominal patient—Unconstrained zero-tracking problem [Colour figure can be viewed at wileyonlinelibrary.com]

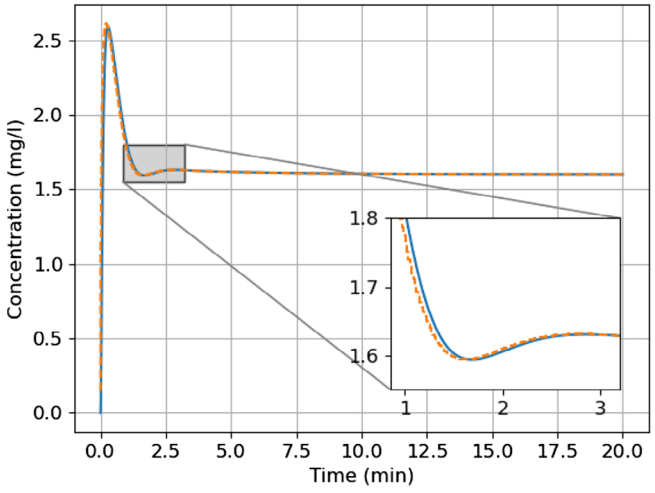

FIGURE 5 Propofol concentration on Effect Compartment for the nominal patient—Unconstrained problem. The magnified part of the figure shows how the observer estimations converge to the actual patient's response [Colour figure can be viewed at wileyonlinelibrary.com]

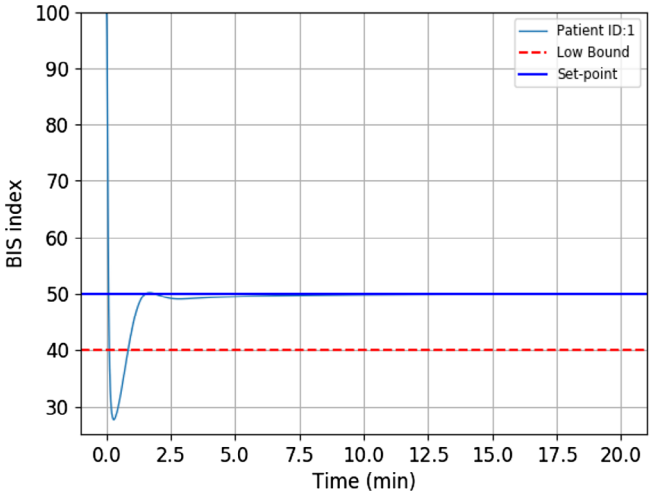

FIGURE 6 BIS index for the nominal patient—Unconstrained problem [Colour figure can be viewed at wileyonlinelibrary.com]

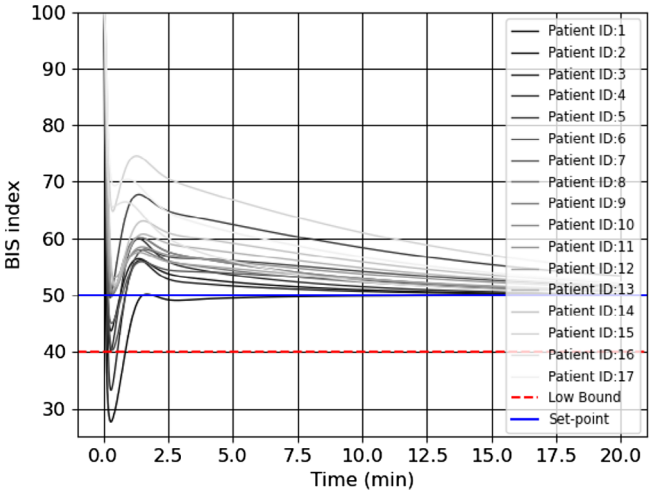

FIGURE 7 BIS Index for all 17 patients—Unconstrained problem [Colour figure can be viewed at wileyonlinelibrary.com]

4.2 | Constrained MPC problem

In this section, we are addressing the problem of Propofol administration for the anesthesia process in the presence of input and output constraints. It is demonstrated that the same control law can be the basis for driving all 17 patients to the desired setpoint while satisfying all constraints. The same administration scheme is adopted for the constrained problem, as depicted in Figure 3. The state observer, at each time instant, is fed with the applied input and the measured output (BIS index), and provides state vector estimations to be used in MPC. The MPC calculates the optimal input (administration rate) to be applied to the patient, and the problem is re-formulated and re-solved at the next time instant.

Target controlled infusion systems, usually make use of syringe pumps with maximum infusion rates between 10 and 160 mg/kg/h.[60] In our simulations, we considered 85 mg/kg/h as the upper bound on the infusion rate, which is converted to u_{max}=200 mg/min (= 3.3 mg/sec), considering a heavy patient weighted 140 kg. It should be noted, however, that the actual infusion rates computed by the controllers are much lower than this bound, which agrees with other observations reported in the literature.[6,30] We also imposed an output constraint, namely the BIS value should be above the lower limit of $BIS = 40$ for all patients during the entire simulation.

Figure 8 presents the optimal drug administration scheme for the constrained problem, while Figure 10 contains the corresponding responses of the BIS index for all 17 patients. We observe that all input and output constraints are satisfied. In particular, the BIS index is above the $BIS = 40$ level, even for the most sensitive patients, who violated this bound in the unconstrained case.

In Figure 9, the Propofol concentration response in the effect compartment is presented. The enlarged region is indicative for the observer's behavior. Like in the unconstrained problem, although initial estimations for Propofol concentration in the effect-site compartment are not highly accurate, they eventually converge to the actual states of the system.

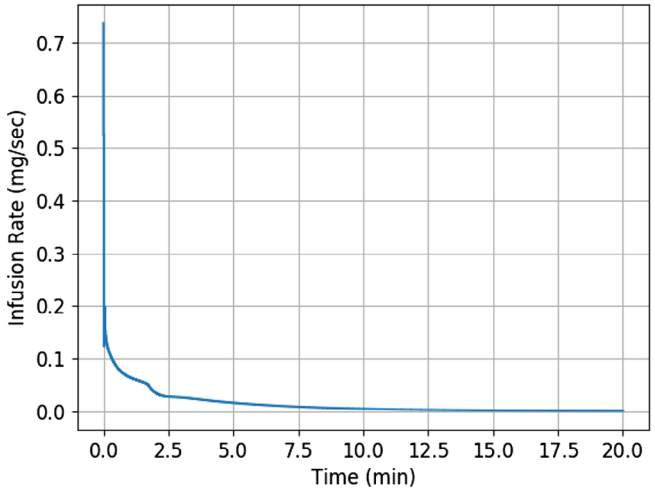

FIGURE 8 Optimal Propofol administration—Constrained zero-tracking problem [Colour figure can be viewed at wileyonlinelibrary.com]

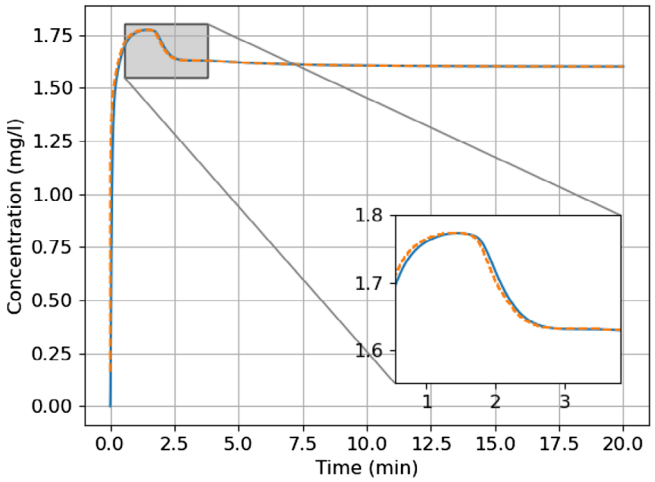

FIGURE 9 Propofol concentration on effect compartment for the nominal patient—Constrained problem. Enlarged detail shows how observer's estimations converge to actual patient's response [Colour figure can be viewed at wileyonlinelibrary.com]

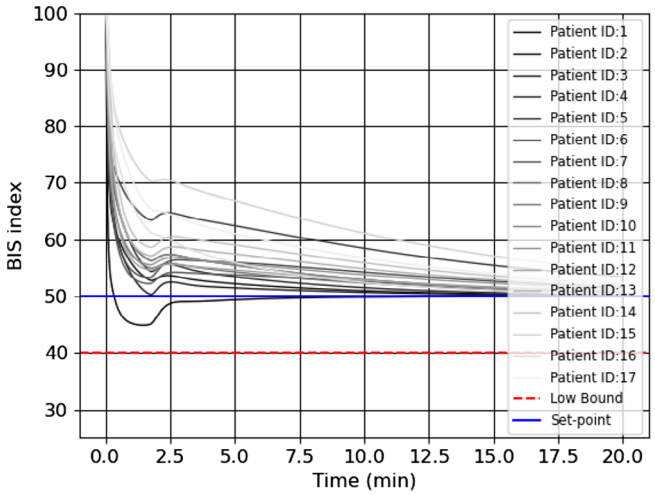

FIGURE 10 BIS index for all 17 patients—Constrained problem [Colour figure can be viewed at wileyonlinelibrary.com]

The *BIS* responses shown in Figure 10 are driven toward the desired setpoint for all 17 patients. The robust controller applies an action (infusion rate) to satisfy simultaneously the requirements of the most sensitive and the less sensitive patient, as well as all the other patients between them. The control law compromises between administering a large enough quantity to drive the insensitive patient close to the $BIS = 50$ index and a smaller quantity to keep the *BIS* index above the lower bound for the sensitive patients. For the less sensitive patients with higher IDs, the responses are slow and need considerable large times to reach steady state. For example, for patient with $ID = 15$, 10 minutes are required to

drive its BIS index below 60, which is usually an acceptable upper bound in Propofol administration. These results are comparable with other studies in the literature.[6,30]

In order to improve the results of the method, we created two smaller groups of patients, while maintaining the configuration of the constrained problem as it has been presented before. The first group contains only the first three most sensitive patients ($ID = 1, 2, 3$). The second group contains the three last patients ($ID = 15, 16, 17$) who are less sensitive to Propofol. The problem is solved for the smaller groups and the results are compared with previous findings, which take simultaneously into account all 17 patients.

The results obtained for the most sensitive group are shown in Figures 11 and 12. For easy comparison, the responses of the same group of patients in the full constrained problem are marked with bold lines in Figure 13. A very small improvement is observed in the responses of the three most sensitive patients when the smaller group is considered in the proposed control scheme.

The results obtained for the least sensitive group are shown in Figures 14 and 15. Figure 16 marks with bold lines the responses of the same group of patients in the full constrained problem. The responses differ significantly between the two figures. More specifically, when the control scheme is applied to the small group of patients, the BIS indices are driven fast to the desired value of $BIS = 50$, thus achieving an improved response.

The above analysis reveals that when a very diverse set of patients is considered in the proposed robust control scheme, the most sensitive patients dominate the determination of the control law. This is because they are the first to violate the low bound of the *BIS* index, when large Propofol infusion rates are used.

By considering smaller groups of patients, we can achieve better performances. In particular, the performance is dramatically improved, when it is applied to groups of the most insensitive patients. In this case, the controller acts more aggressively by delivering larger amounts of drug and therefore achieving faster settling times.

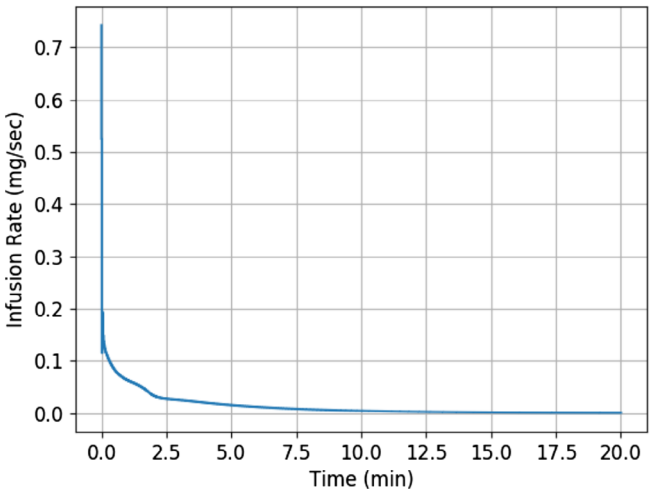

FIGURE 11 Optimal Propofol adminstration for patients with $ID = 1, 2, 3$—Constrained zero-tracking problem [Colour figure can be viewed at wileyonlinelibrary.com]

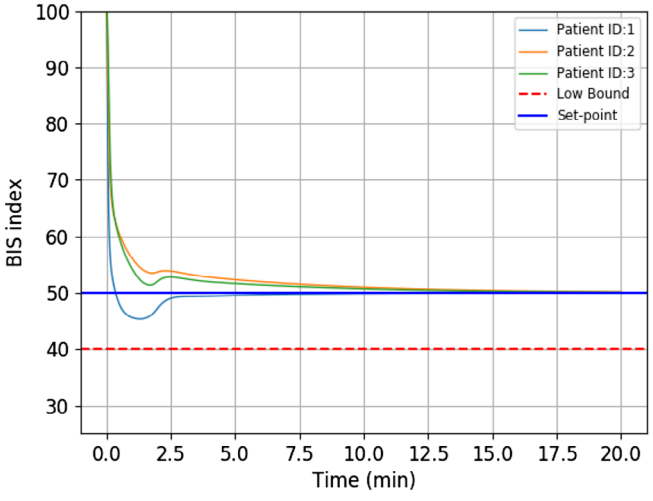

FIGURE 12 BIS index for patients with $ID = 1, 2, 3$—Constrained problem [Colour figure can be viewed at wileyonlinelibrary.com]

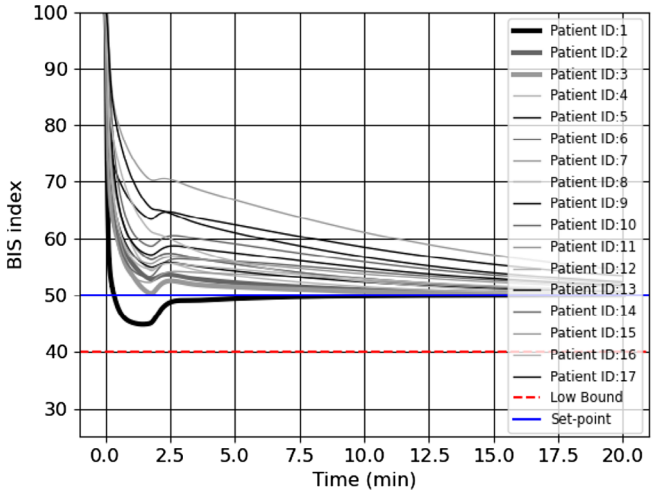

FIGURE 13 BIS index for all 17 patients. In bold patients with $ID = 1, 2, 3$—Constrained problem [Colour figure can be viewed at wileyonlinelibrary.com]

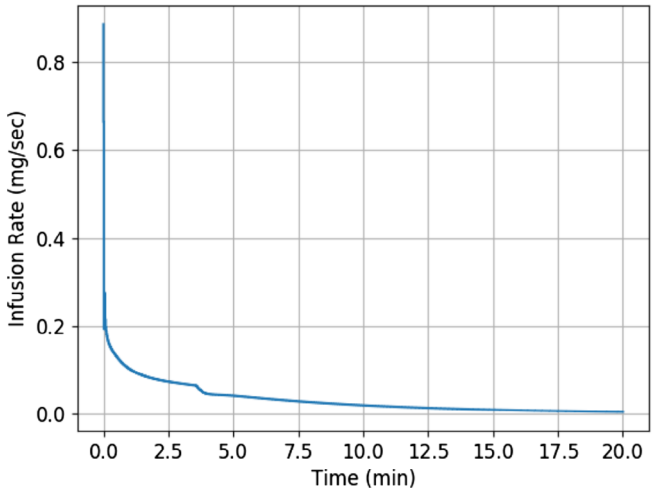

FIGURE 14 Optimal Propofol administration for patients with $ID = 15, 16, 17$—Constrained zero-tracking problem [Colour figure can be viewed at wileyonlinelibrary.com]

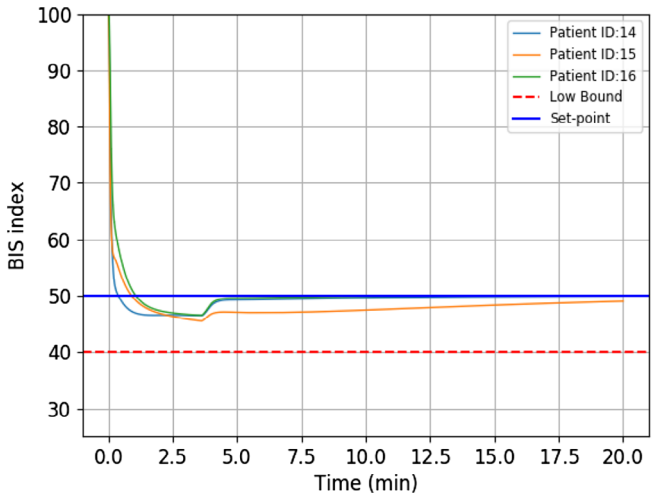

FIGURE 15 BIS index for patients with $ID = 15, 16, 17$—Constrained problem [Colour figure can be viewed at wileyonlinelibrary.com]

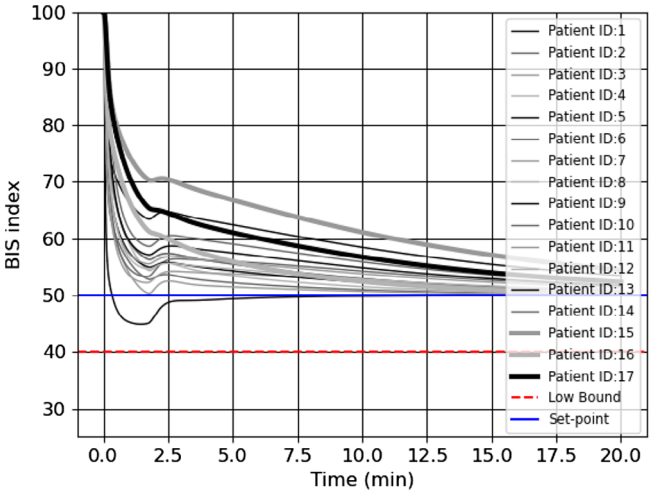

FIGURE 16 BIS index for all 17 patients. In bold patients with $ID = 15, 16, 17$—Constrained problem [Colour figure can be viewed at wileyonlinelibrary.com]

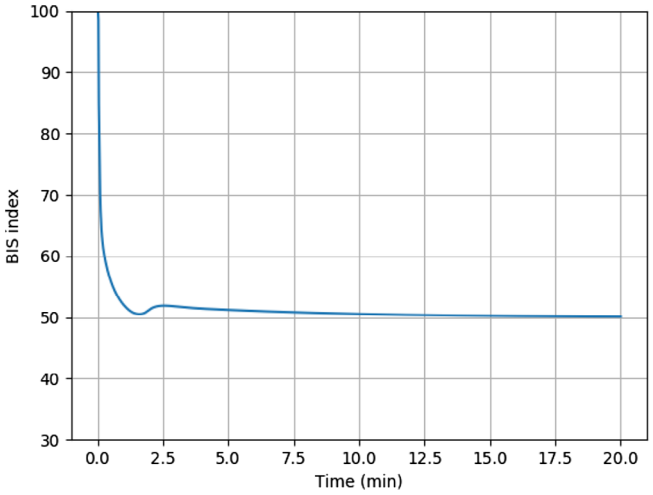

FIGURE 17 BIS index evolution during induction phase for a new patient [Colour figure can be viewed at wileyonlinelibrary.com]

4.3 | New patient

In this section, the treatment of a new patient is presented, using the control laws calculated for the 17 original patients. The matrices describing the dynamics of this patient are shown in Appendix B. It is easy to verify that this patient belongs to the convex hull of the 17 original patients, and to the convex hull of the group of sensitive patients ($ID = 1, 2, 3$). The same constraints are imposed regarding the input and the output of the system, as in previous simulations. We will examine the performance of the MPC control scheme both during the induction phase, to verify that the controller drives the patient to the desired setpoint with respect to the imposed constraints, and the maintenance phase, to verify that the controller is able to maintain the desired level of anesthesia, regardless of the disturbances that may occur during a typical surgery.

4.3.1 | Induction phase

The goal is to bring the patient in the desired depth of anesthesia rapidly, so that the process is not detrimental and painful for the patient and the surgeon can start the operation as soon as possible.[6] In order to achieve the desired state, his/her BIS index should fall to the level of 50 without much undershoot, that is, BIS values below 30 should be avoided. The response of the BIS index after applying the MPC controller designed for the group of sensitive patients is shown in Figure 17. The controller is able to drive the patient to the desired level of anesthesia in less than 2 minutes, smoothly and without an undershoot.

4.3.2 | Maintenance phase

Besides ensuring proper performance during induction phase, it is essential to also guarantee that the controller maintains the BIS index value within the desired bounds, that is, is capable of rejecting any disturbances, during the entire surgery. In order to examine the performance of the controller during the maintenance phase, a realistic scenario of disturbances is defined, trying to mimic typical surgery stimuli that may happen in an operation theater, similar to References 6 and 30. The scenario consists of different phases, each one representing a change in measured BIS index due to various reasons as shown in Table 1. It is assumed that the patient has passed successfully the induction phase achieving the desired setpoint of BIS index equal to 50; therefore, the time axis starts at a later time instance.

In Figure 18, the evolution of BIS index according to the scenario of Table 1 is presented. It can be seen that the controller in all phases of the scenario manages to return rapidly the BIS index of the patient back to the desired setpoint.

In Figure 19, the corresponding administration rate is depicted. To achieve rapid responses of the BIS values back to the desired levels, the controller initially delivers large quantities of Propofol (similar to bolus administration) and then behaves smoother to avoid oscillations, until reaching the desired BIS value.

4.4 | Computational aspects

All simulations were performed in Python in a Macbook Pro (version 10.13.6, 2.66 GHz Intel Core 2 Duo, 4 GB RAM) running Mac OS Sierra. For a single patient, as in case of Section 4.3.1, at each time instant the MPC optimization problem was formulated and solved—on average—in 0.21 seconds, while the total simulation time was equal to 251 seconds. The

TABLE 1 Stimuli scenario during maintenance phase

Phase	Time	BIS	Reason
Start	60	50	Start of maintenance phase
A	70	70	Intubation
B	80	70	Surgical incision
C	86	30	No surgical stimulus (i.e., waiting for pathology result)
D	90	70	Onset of a continuous normal surgical stimulation
E	100	60	
F	105	80	
G	110	60	Short-lasting stimulation within the surgical period
H	115	80	
I	125	60	
End	150	50	Withdrawal of stimulation during the closing period

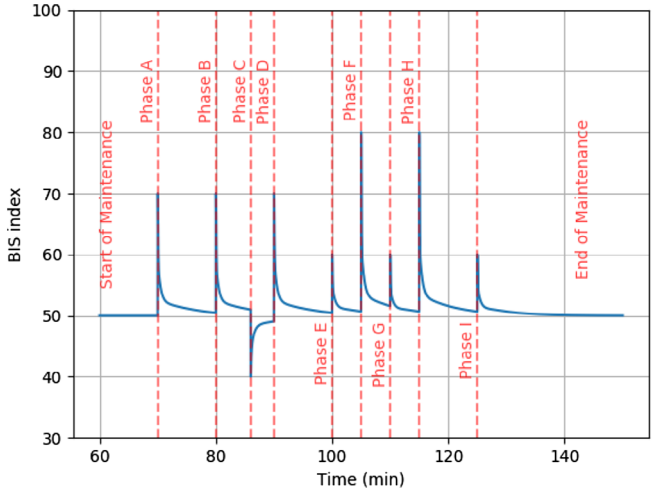

FIGURE 18 BIS index evolution according to stimuli scenario for new patient—Disturbance rejection problem [Colour figure can be viewed at wileyonlinelibrary.com]

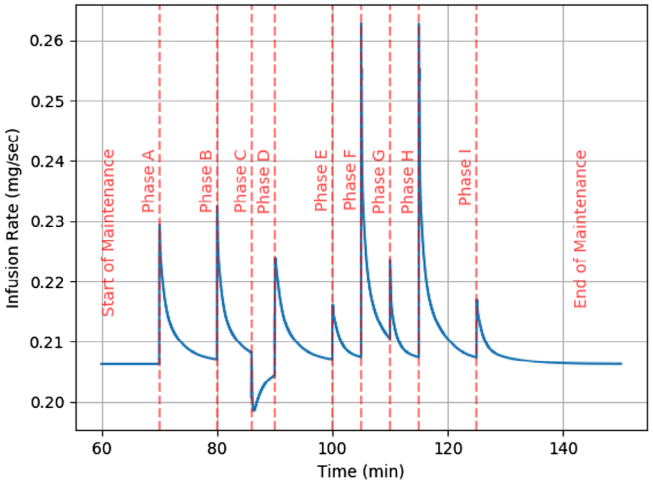

FIGURE 19 Evolution of administration rate of Propofol according to stimuli scenario for new patient—Disturbance rejection problem [Colour figure can be viewed at wileyonlinelibrary.com]

maximum time for solving the MPC problem at a time instant was 0.27 seconds. For the formulation of the optimization algorithm, CVXPY was used. CVXPY is a Python-embedded modeling language for convex optimization problems.[61,62] The solver used for the solution of the optimization problems was CVXOPT,[63,64] using function *sdp* for semidefinite programming which acts as an interface to *conelp* for cone programs with no second-order cone constraints.

5 | CONCLUSIONS

In this work, we presented a robust MPC application based on LMIs for the control of the administration of Propofol, which is a widely used agent for anesthesia. The only measurable quantity is considered to be the BIS index, that is, the output of the system, so no knowledge about the state of the system is available. To address this issue, a state observer is used in order to compute accurate estimates of the state vector of the system. We illustrated that the proposed methodology was able to compute a control law, that drives the *BIS* index to the desired set point for different patients, while satisfying the constraints. The dynamic characteristics of the responses were improved when considering smaller groups of similar patients. This defines a classification problem that will be addressed in a future work, that is, the selection of the most suitable among many pharmacokinetic models based on macroscopic characteristics of the patient, such as age, height, weight, and gender.

DATA AVAILABILITY STATEMENT

The data that support the findings of this study are available in Ionescu C.M., Nascu I., De Keyser R. (2011) Robustness Tests of a Model Based Predictive Control Strategy for Depth of Anesthesia Regulation in a Propofol to Bispectral Index Framework. In: Vlad S., Ciupa R.V. (eds) International Conference on Advancements of Medicine and Health Care through Technology. IFMBE Proceedings, vol 36. Springer, Berlin, Heidelberg at https://doi.org/10.1007/978-3-642-22586-4_50, reference number 6.

ORCID

Haralambos Sarimveis https://orcid.org/0000-0002-8607-9965

REFERENCES

1. Absalom AR, De Keyser R, Struys MM. Closed loop anesthesia: are we getting close to finding the holy grail? *Anesth Analg*. 2011;112(3):516-518. https://doi.org/10.1213/ANE.0b013e318203f5ad.
2. Fuentes-Gari M, Velliou E, Misener R, et al. A systematic framework for the design, simulation and optimization of personalized healthcare: making and healing blood. *Comput Chem Eng*. 2015;81:80-93.Special Issue: Selected papers from the 8th International Symposium on the Foundations of Computer-Aided Process Design (FOCAPD 2014), July 13-17, 2014, Cle Elum, Washington, DC. https://doi.org/10.1016/j.compchemeng.2015.03.008.
3. Morley A, Derrick J, Mainland P, Lee B, Short T. Closed loop control of anaesthesia: an assessment of the bispectral index as the target of control. *Anaesthesia*. 2000;55(10):953-959. https://doi.org/10.1046/j.1365-2044.2000.01527.x.
4. Naşcu I, Krieger A, Ionescu CM, Pistikopoulos EN. Advanced model-based control studies for the induction and maintenance of intravenous anaesthesia. *IEEE Trans Biomed Eng*. 2014;62(3):832-841. https://doi.org/10.1109/TBME.2014.2365726.

5. Ionescu CM, Hodrea R, De Keyser R. Variable time-delay estimation for anesthesia control during intensive care. *IEEE Trans Biomed Eng*. 2011;58(2):363-369. https://doi.org/10.1109/TBME.2010.2088121.
6. Ionescu CM, Nascu I, De Keyser R. Robustness tests of a model based predictive control strategy for depth of anesthesia regulation in a propofol to bispectral index framework. Paper presented at: Proceedings of the International Conference on Advancements of Medicine and Health Care through Technology; 2011:234-239; Springer, Berlin, Heidelberg/Germany.
7. Neckebroek MM, De Smet T, Struys MM. Automated drug delivery in anesthesia. *Current Anesthesiol Rep*. 2013;3(1):18-26. https://doi.org/10.1007/s40140-012-0004-3.
8. Dumont GA. Closed-loop control of anesthesia-a review. *IFAC Proc Vols*. 2012;45(18):373-378.8th IFAC Symposium on Biological and Medical Systems. https://doi.org/10.3182/20120829-3-HU-2029.00102.
9. Bibian S. Automation in Clinical Anesthesia [PhD thesis]. University of British Columbia; 2006
10. Sakai T, Matsuki A, White P, Giesecke A. Use of an EEG-bispectral closed-loop delivery system for administering propofol. *Acta Anaesthesiol Scand*. 2000;44(8):1007-1010. https://doi.org/10.1034/j.1399-6576.2000.440819.x.
11. Absalom AR, Sutcliffe N, Kenny GN. Closed-loop control of anesthesia using bispectral indexperformance assessment in patients undergoing major orthopedic surgery under combined general and regional anesthesia. *Anesthesiol J Am Soc Anesthesiol*. 2002;96(1):67-73. https://doi.org/10.1097/00000542-200201000-00017.
12. Absalom AR, Kenny G. Closed-loop control of propofol anaesthesia using bispectral index$^{\texttrademark}$: performance assessment in patients receiving computer-controlled propofol and manually controlled remifentanil infusions for minor surgery. *Br J Anaesth*. 2003;90(6):737-741. https://doi.org/10.1097/00000542-200201000-00017.
13. Merigo L, Beschi M, Padula F, Latronico N, Paltenghi M, Visioli A. Event-based control of depth of hypnosis in anesthesia. *Comput Methods Prog Biomed*. 2017;147:63-83. https://doi.org/10.1016/j.cmpb.2017.06.007.
14. Contreras I, Quirós C, Giménez M, Conget I, Vehi J. Profiling intra-patient type I diabetes behaviors. *Comput Methods Prog Biomed*. 2016;136:131-141. https://doi.org/10.1016/j.cmpb.2016.08.022.
15. Soltesz K, Hahn JO, Hägglund T, Dumont GA, Ansermino JM. Individualized closed-loop control of propofol anesthesia: a preliminary study. *Biomed Signal Process Control*. 2013;8(6):500-508. https://doi.org/10.1016/j.bspc.2013.04.005.
16. Curatolo M, Derighetti M, Petersen-Felix S, Feigenwinter P, Fischer M, Zbinden A. Fuzzy logic control of inspired isoflurane and oxygen concentrations using minimal flow anaesthesia. *British J Anaesthesia*. 1996;76(2):245-250. https://doi.org/10.1093/bja/76.2.245.
17. Haddad WM, Hayakawa T, Bailey JM. Nonlinear adaptive control for intensive care unit sedation and operating room hypnosis. Paper presented at: Proceedings of the 2003 IEEE American Control Conference. Denver, CO; 2003;2:1808-1813.
18. Khodaei MJ, Mehrvarz A, Jalili N. An adaptive multi-critic neuro-fuzzy control framework for intravenous anesthesia administration. *IFAC-PapersOnLine*. 2019;51(34):202-207.2nd IFAC Conference on Cyber-Physical and Human Systems CPHS 2018. https://doi.org/10.1016/j.ifacol.2019.01.066.
19. Navarro-Guerrero G, Tang Y. Fractional order model reference adaptive control for anesthesia. *Int J Adapt Control Signal Process*. 2017;31(9):1350-1360. https://doi.org/10.1002/acs.2769.
20. Merigo L, Padula F, Pawlowski A, et al. A model-based control scheme for depth of hypnosis in anesthesia. *Biomed Signal Process Control*. 2018;42:216-229. https://doi.org/10.1016/j.bspc.2018.01.023.
21. Ionescu CM, De Keyser R, Torrico BC, De Smet T, Struys MM, Normey-Rico JE. Robust predictive control strategy applied for propofol dosing using BIS as a controlled variable during anesthesia. *IEEE Trans Biomed Eng*. 2008;55(9):2161-2170. https://doi.org/10.1109/TBME.2008.923142.
22. Savoca A, Manca D. A physiologically-based approach to model-predictive control of anesthesia and analgesia. *Biomed Signal Process Control*. 2019;53:101553. https://doi.org/10.1016/j.bspc.2019.04.030.
23. Ingole D, Drgoňa J, Kvasnica M. Offset-free hybrid model predictive control of bispectral index in anesthesia. Paper presented at: Proceedings of the 2017 21st International Conference on Process Control (PC). Strbske Pleso; 2017:422-427; IEEE.
24. Eskandari N, van Heusden K, Dumont GA. Extended habituating model predictive control of propofol and remifentanil anesthesia. *Biomed Signal Process Control*. 2020;55:101656. https://doi.org/10.1016/j.bspc.2019.101656.
25. Gholami B, Haddad WM, Bailey JM, Tannenbaum AR. Optimal drug dosing control for intensive care unit sedation by using a hybrid deterministic–stochastic pharmacokinetic and pharmacodynamic model. *Opt Control Appl Methods* 2013;34(5):547–561. https://doi.org/10.1002/oca.2038
26. Sadati N, Hosseinzadeh M, Dumont GA. Multi-model robust control of depth of hypnosis. *Biomed Signal Process Control*. 2018;40:443-453. https://doi.org/10.1016/j.bspc.2017.10.003.
27. Kothare MV, Balakrishnan V, Morari M. Robust constrained model predictive control using linear matrix inequalities. *Automatica*. 1996;32(10):1361-1379. https://doi.org/10.1016/0005-1098(96)00063-5.
28. Padula F, Ionescu C, Latronico N, Paltenghi M, Visioli A, Vivacqua G. Optimized PID control of depth of hypnosis in anesthesia. *Comput Methods Prog Biomed*. 2017;144:21-35. https://doi.org/10.1016/j.cmpb.2017.03.013.
29. Yelneedi S, Samavedham L, Rangaiah G. Advanced control strategies for the regulation of hypnosis with propofol. *Ind Eng Chem Res*. 2009;48(8):3880-3897. https://doi.org/10.1021/ie800695b.
30. Naşcu I, Pistikopoulos EN. Modeling, estimation and control of the anaesthesia process. *Comput Chem Eng*. 2017;107:318-332.In honor of Professor Rafiqul Gani doi. https://doi.org/10.1016/j.compchemeng.2017.02.016.
31. Dua P, Dua V, Pistikopoulos EN. Modelling and multi-parametric control for delivery of anaesthetic agents. *Med Biol Eng Comput*. 2010;48(6):543-553. https://doi.org/10.1007/s11517-010-0604-3.
32. Naşcu I, Oberdieck R, Pistikopoulos EN. Explicit hybrid model predictive control strategies for intravenous anaesthesia. *Comput Chem Eng*. 2017;106:814-825. https://doi.org/10.1016/j.compchemeng.2017.01.033.

33. Nascu I, Lambert RS, Pistikopoulos EN. A combined estimation and multi-parametric model predictive control approach for intravenous anaesthesia. Paper presented at: Proceedings of the 2014 IEEE International Conference on Systems, Man, and Cybernetics (SMC). San Diego, CA; 2014:2458-2463.
34. Krieger A, Pistikopoulos EN. Model predictive control of anesthesia under uncertainty. *Comput Chem Eng*. 2014;71:699-707. https://doi.org/10.1016/j.compchemeng.2014.07.025.
35. Wu A, Wang Y, Min S, Liu H, Xie F. Etomidate-loaded micelles for short-acting general anesthesia: preparation, characterizations and in vivo studies. *J Drug Deliv Sci Technol*. 2018;46:156-161. https://doi.org/10.1016/j.jddst.2018.05.013.
36. Liu H, Zhou X, Wang Y, Yang M, Xu X, Wu A. Mixed micelle as nanocarrier for etomidate: development, in vitro characterizations, and in vivo study on toxicity and anesthetic effects. *J Drug Deliv Sci Technol*. 2019;49:123-131. https://doi.org/10.1016/j.jddst.2018.10.038.
37. Struys MM, Jensen EW, Smith W, et al. Performance of the ARX-derived auditory evoked potential index as an indicator of anesthetic deptha comparison with bispectral index and hemodynamic measures during propofol administration. *Anesthesiol J Am Soc Anesthesiol*. 2002;96(4):803-816. https://doi.org/10.1097/00000542-200204000-00006.
38. Chang TG, Smith JR, Principe JC. An expert system for multichannel sleep EEG/EOG signal analysis. *ISA Trans*. 1989;28(1):45-51. https://doi.org/10.1016/0019-0578(89)90056-6.
39. Johansen JW. Update on bispectral index monitoring. *Best Pract Res Clin Anaesthesiol*. 2006;20(1):81-99.Monitoring Consciousness. https://doi.org/10.1016/j.bpa.2005.08.004.
40. Marsh B, White M, Morton N, Kenny G. Pharmacokinetic model driven infusion of propofol in children. *BJA*. 1991;67(1):41-48. https://doi.org/10.1093/bja/67.1.41.
41. Nunes CS, Mendonça T, Lemos JM, Amorim P. Feedforward adaptive control of the bispectral index of the EEG using the intravenous anaesthetic drug propofol. *Int J Adapt Control Signal Process*. 2009;23(5):485-503. https://doi.org/10.1002/acs.1097.
42. Schnider TW, Minto CF, Gambus PL, et al. The influence of method of administration and covariates on the pharmacokinetics of propofol in adult volunteers. *Anesthesiol J Am Soc Anesthesiol*. 1998;88(5):1170-1182. https://doi.org/10.1097/00000542-199805000-00006.
43. Schnider TW, Minto CF, Shafer SL, et al. The influence of age on propofol pharmacodynamics. *Anesthesiol J Am Soc Anesthesiol*. 1999;90(6):1502-1516. https://doi.org/10.1097/00000542-199906000-00003.
44. Bibian S, Ries CR, Huzmezan M, Dumont G. Introduction to automated drug delivery in clinical anesthesia. *Eur J Control*. 2005;11(6):535-557. https://doi.org/10.3166/ejc.11.535-557.
45. Struys MM, Vereecke H, Moerman A, et al. Ability of the bispectral index, autoregressive modelling with exogenous input-derived auditory evoked potentials, and predicted propofol concentrations to measure patient responsiveness during anesthesia with propofol and remifentanil. *Anesthesiol J Am Soc Anesthesiol*. 2003;99(4):802-812. https://doi.org/10.1097/00000542-200310000-00010.
46. The Scipy Community. scipy.signal.cont2discrete - SciPy v.1.6.0 Reference Guide; 2014. https://docs.scipy.org/doc/scipy/reference/generated/scipy.signal.cont2% discrete.html?highlight=cont2discrete#scipy.signal.cont2discrete. Online. Accessed January 23, 2021.
47. Huang G, Wang S. Use of uncertainty polytope to describe constraint processes with uncertain time-delay for robust model predictive control applications. *ISA Trans*. 2009;48(4):503-511. https://doi.org/10.1016/j.isatra.2009.06.002.
48. Razi M, Haeri M. Design of a robust model predictive controller with reduced computational complexity. *ISA Trans*. 2014;53(6):1754-1759. https://doi.org/10.1016/j.isatra.2014.09.008.
49. Wan Z, Kothare MV. Robust output feedback model predictive control using off-line linear matrix inequalities. *J Process Control*. 2002;12(7):763-774. https://doi.org/10.1016/S0959-1524(02)00003-3.
50. Wan Z, Kothare MV. Efficient robust constrained model predictive control with a time varying terminal constraint set. *Syst Control Lett*. 2003;48(5):375-383. https://doi.org/10.1016/S0167-6911(02)00291-8.
51. Wan Z, Pluymers B, Kothare MV, De Moor B. Comments on: εEfficient robust constrained model predictive control with a time varying terminal constraint setε by Wan and Kothare. *Syst Control Lett*. 2006;55(7):618-621. https://doi.org/10.1016/j.sysconle.2006.02.006.
52. Nath A, Dey R. Robust guaranteed-cost output feedback control of blood glucose in type 1 diabetes patient with intrapatient variability. *Opt Control Appl Methods*. 2020;41(5):1422-1438. https://doi.org/10.1002/oca.2607.
53. Boyd S, El Ghaoui L, Feron E, Balakrishnan V. *Linear Matrix Inequalities in System and Control Theory*. Vol 15. Philadelphia, Pennsylvania: SIAM; 1994.
54. Minh VT, Bin Mohd Hashim F. Robust model predictive control schemes for tracking setpoints. *J Control Sci Eng*. 2010;2010(649461):9. https://doi.org/10.1155/2010/649461.
55. Sopasakis P, Patrinos P, Sarimveis H. Robust model predictive control for optimal continuous drug administration. *Comput Methods Prog Biomed*. 2014;116(3):193-204. https://doi.org/10.1016/j.cmpb.2014.06.003.
56. Batmani Y, Khaloozadeh H. Optimal chemotherapy in cancer treatment: state dependent Riccati equation control and extended Kalman filter. *Opt Control Appl Methods*. 2013;34(5):562-577. https://doi.org/10.1002/oca.2039.
57. Rezvanian S, Towhidkhah F, Ghahramani N. Controlling the depth of anesthesia using model predictive controller and extended Kalman filter. Paper presented at: Proceedings of the 2011 1st Middle East Conference on Biomedical Engineering. Sharjah, United Arab Emirates; 2011:213-216; IEEE.
58. Kalman RE. A new approach to linear filtering and prediction problems. *J Basic Eng*. 1960;82(1):35-45. https://doi.org/10.1115/1.3662552.
59. Straw AD. Kalman filtering; February 23, 2020. https://scipy-cookbook.readthedocs.io/items/KalmanFiltering.html Online. Accessed January 23, 2021.
60. Simoni RF, LEDPG M, Esteves LO, et al. Comparative study between fast and slow induction of propofol given by target-controlled infusion: expected propofol concentration at the effect site. randomized controlled trial. *Braz J Anesthesiol*. 2015;65(2):99-103. https://doi.org/10.1016/j.bjane.2013.07.015.

61. Diamond S, Boyd S. CVXPY: a Python-embedded modeling language for convex optimization. *J Mach Learn Res*. 2016;17(83):1-5.
62. Agrawal A, Verschueren R, Diamond S, Boyd S. A rewriting system for convex optimization problems. *J Control Decis*. 2018;5(1):42-60.
63. Andersen MS Dahl J, Vandenberghe L. CVXOPT: a python package for convex optimization cvxoptorg; vol. 1, 2018:2.
64. Andersen MS, Dahl J, Vandenberghe L. CVXOPT: a python package for convex optimization. abel. ee. ucla. edu/cvxopt; 2013:88.

How to cite this article: Ntouskas S, Sarimveis H. A robust model predictive control framework for the regulation of anesthesia process with Propofol. *Optim Control Appl Meth*. 2021;1–22. https://doi.org/10.1002/oca.2710

APPENDIX A

Here we provide the matrices A and B for all 17 patients of the dataset that define set Ω and matrix C. Matrix C is the same for all the patients of the dataset, and equal to:

$$C = \begin{bmatrix} 0 & 0 & 0 & 1 \end{bmatrix}.$$

Matrices A and B are formulated after equations 1 in continuous time. Next, state space system is discretized by using function `cont2discrete` contained in library `scipy`.[46] The selected method for the discretization was the *zero-order hold*.

$$A_1 = \begin{bmatrix} 0.394 & 0.181 & 0.01304 & 0 \\ 0.221 & 0.751 & 0.00282 & 0 \\ 0.0994 & 0.0176 & 0.981 & 0 \\ 0.485 & 0.1277 & 0.00876 & 0.10076 \end{bmatrix}$$

$$B_1 = \begin{bmatrix} 3.1996 & 0.6882 & 0.2881 & 2.1423 \end{bmatrix}^T$$

$$A_2 = \begin{bmatrix} 0.206 & 0.089 & 0.00999 & 0 \\ 0.302 & 0.852 & 0.0041 & 0 \\ 0.127 & 0.015 & 0.981 & 0 \\ 0.2927 & 0.0465 & 0.005 & 0.3027 \end{bmatrix}$$

$$B_2 = \begin{bmatrix} 2.453 & 1.0 & 0.4005 & 1.2287 \end{bmatrix}^T$$

$$A_3 = \begin{bmatrix} 0.242 & 0.0955 & 0.0107 & 0 \\ 0.259 & 0.8457 & 0.0034 & 0 \\ 0.1085 & 0.01285 & 0.981 & 0 \\ 0.318 & 0.049 & 0.0053 & 0.3027 \end{bmatrix}$$

$$B_3 = \begin{bmatrix} 2.624 & 0.8392 & 0.3358 & 1.293 \end{bmatrix}^T$$

$$A_4 = \begin{bmatrix} 0.206 & 0.089 & 0.0099 & 0 \\ 0.3022 & 0.8512 & 0.0041 & 0 \\ 0.1268 & 0.0153 & 0.981 & 0 \\ 0.2927 & 0.0466 & 0.005 & 0.3027 \end{bmatrix}$$

$$B_4 = \begin{bmatrix} 2.453 & 1.0 & 0.4005 & 1.228 \end{bmatrix}^T$$

$$A_5 = \begin{bmatrix} 0.344 & 0.1112 & 0.00747 & 0 \\ 0.2265 & 0.84 & 0.0017 & 0 \\ 0.158 & 0.0178 & 0.988 & 0 \\ 0.4495 & 0.0778 & 0.0051 & 0.10076 \end{bmatrix}$$

$$B_5 = \begin{bmatrix} 3.0395 & 0.697 & 0.466 & 2.06 \end{bmatrix}^T$$

$$A_6 = \begin{bmatrix} 0.3933 & 0.1812 & 0.00786 & 0 \\ 0.2214 & 0.751 & 0.0017 & 0 \\ 0.0998 & 0.0176 & 0.988 & 0 \\ 0.4624 & 0.1122 & 0.0046 & 0.1746 \end{bmatrix}$$

$$B_6 = \begin{bmatrix} 3.199 & 0.688 & 0.289 & 1.874 \end{bmatrix}^T$$

$$A_7 = \begin{bmatrix} 0.2666 & 0.1515 & 0.00664 & 0 \\ 0.2468 & 0.758 & 0.0020 & 0 \\ 0.0843 & 0.0156 & 0.988 & 0 \\ 0.3809 & 0.1111 & 0.0046 & 0.1007 \end{bmatrix}$$

$$B_7 = \begin{bmatrix} 2.704 & 0.815 & 0.257 & 1.874 \end{bmatrix}^T$$

$$A_8 = \begin{bmatrix} 0.286 & 0.131 & 0.00913 & 0 \\ 0.266 & 0.802 & 0.0028 & 0 \\ 0.116 & 0.0175 & 0.985 & 0 \\ 0.3854 & 0.0828 & 0.0055 & 0.175 \end{bmatrix}$$

$$B_8 = \begin{bmatrix} 2.793 & 0.855 & 0.351 & 1.6889 \end{bmatrix}^T$$

$$A_9 = \begin{bmatrix} 0.286 & 0.131 & 0.00913 & 0 \\ 0.266 & 0.802 & 0.0028 & 0 \\ 0.116 & 0.0175 & 0.985 & 0 \\ 0.344 & 0.0667 & 0.0044 & 0.303 \end{bmatrix}$$

$$B_9 = \begin{bmatrix} 2.793 & 0.855 & 0.351 & 1.353 \end{bmatrix}^T$$

$$A_{10} = \begin{bmatrix} 0.286 & 0.131 & 0.00913 & 0 \\ 0.266 & 0.802 & 0.0028 & 0 \\ 0.116 & 0.0175 & 0.985 & 0 \\ 0.344 & 0.0667 & 0.0044 & 0.303 \end{bmatrix}$$

$$B_{10} = \begin{bmatrix} 2.793 & 0.855 & 0.351 & 1.353 \end{bmatrix}^T$$

$$A_{11} = \begin{bmatrix} 0.393 & 0.1812 & 0.00786 & 0 \\ 0.2214 & 0.751 & 0.00169 & 0 \\ 0.0998 & 0.0176 & 0.988 & 0 \\ 0.485 & 0.1277 & 0.0053 & 0.1008 \end{bmatrix}$$

$$B_{11} = \begin{bmatrix} 3.1989 & 0.688 & 0.289 & 2.142 \end{bmatrix}^T$$

$$A_{12} = \begin{bmatrix} 0.2667 & 0.1515 & 0.00664 & 0 \\ 0.2247 & 0.758 & 0.00201 & 0 \\ 0.084 & 0.0156 & 0.988 & 0 \\ 0.369 & 0.0981 & 0.0041 & 0.175 \end{bmatrix}$$

$$B_{12} = \begin{bmatrix} 2.704 & 0.815 & 0.257 & 1.646 \end{bmatrix}^T$$

$$A_{13} = \begin{bmatrix} 0.3933 & 0.1812 & 0.00786 & 0 \\ 0.2214 & 0.751 & 0.00169 & 0 \\ 0.0998 & 0.0176 & 0.988 & 0 \\ 0.4067 & 0.0901 & 0.0037 & 0.3027 \end{bmatrix}$$

$$B_{13} = \begin{bmatrix} 3.1989 & 0.688 & 0.289 & 1.497 \end{bmatrix}^T$$

$$A_{14} = \begin{bmatrix} 0.3933 & 0.1812 & 0.00786 & 0 \\ 0.2214 & 0.751 & 0.00169 & 0 \\ 0.0998 & 0.0176 & 0.988 & 0 \\ 0.4067 & 0.0901 & 0.0037 & 0.3027 \end{bmatrix}$$

$$B_{14} = \begin{bmatrix} 3.1989 & 0.688 & 0.289 & 1.497 \end{bmatrix}^T$$

$$A_{15} = \begin{bmatrix} 0.344 & 0.1112 & 0.00747 & 0 \\ 0.226 & 0.84 & 0.00172 & 0 \\ 0.158 & 0.0178 & 0.989 & 0 \\ 0.381 & 0.055 & 0.0035 & 0.3027 \end{bmatrix}$$

$$B_{15} = \begin{bmatrix} 3.0395 & 0.697 & 0.466 & 1.443 \end{bmatrix}^T$$

$$A_{16} = \begin{bmatrix} 0.206 & 0.089 & 0.00999 & 0 \\ 0.302 & 0.852 & 0.0041 & 0 \\ 0.1268 & 0.015 & 0.981 & 0 \\ 0.323 & 0.0577 & 0.0062 & 0.175 \end{bmatrix}$$

$$B_{16} = \begin{bmatrix} 2.453 & 1.0 & 0.4005 & 1.528 \end{bmatrix}^T.$$

APPENDIX B

This Appendix provides numerical information regarding the new patient of Section 4.3. Matrices A and B are selected in continuous time. Next, state space system is discretized by using function `cont2discrete`contained in library `scipy`.[46] The selected method for the discretization was the *zero-order hold*.

$$A = \begin{bmatrix} 0.2706 & 0.1186 & 0.01114 & 0. \\ 0.2635 & 0.8162 & 0.0034 & 0. \\ 0.1132 & 0.0159 & 0.981 & 0. \\ 0.3653 & 0.0711 & 0.0064 & 0.2089 \end{bmatrix}$$

$$B = \begin{bmatrix} 2.7352 \\ 0.8492 \\ 0.3452 \\ 1.5654 \end{bmatrix}.$$